Available online at www.sciencedirect.com
ScienceDirect
Earth and Planetary Science Letters 250 (2006) 27–37
EPSL
www.elsevier.com/locate/epsl

How accurately can NRM/SIRM determine the ancient planetary magnetic field intensity?

Yongjae Yu

Geosciences Research Division, Scripps Institution of Oceanography, La Jolla, CA 92093-0220, USA

Received 24 January 2006; received in revised form 11 July 2006; accepted 14 July 2006
Available online 17 August 2006
Editor: S. King

Abstract

The present study tested grain-size dependence of thermoremanent magnetization (TRM)/saturation isothermal remanent magnetization (SIRM) as well as its stability against demagnetization. The TRM/SIRM ratio is dependent on the grain-size of magnetite, suggesting that a strong constraint on grain-size characterization is necessary to be used as a paleointensity proxy in planetary magnetism. In addition, the TRM/SIRM ratio increases as the alternating-field increases for fine-grained magnetite. Accuracy of TRM/SIRM was investigated using historic Showa lava erupted in 1946. It was observed that the natural remanent magnetization (NRM)/SIRM ratio of 0.032 is comparable to the field intensity of 46.80 μT. However, the uncertainty of NRM/SIRM was an order of magnitude larger than that of the companion Thellier estimation. Therefore, the NRM/SIRM ratio can only provide crude estimations on the absolute planetary magnetic field intensity. In practice, anisotropy correction is advisable to reduce the scatter of NRM/SIRM.

Keywords: paleointensity; NRM/SIRM; meteorite; magnetite; anisotropy correction

1. Introduction

Information on the intensity of ancient planetary magnetic field is a first-order constraint on the formation and evolution of planets and asteroids in solar system. On Earth, ancient geomagnetic field intensity (paleointensity in abbreviation) determination has broad applications from chronology to discussions regarding regimes of convection in the outer-core, the growth of inner-core, and possibly the evolution of core–mantle boundary. Despite such importance, data constraining the past intensity of the planetary body remain relatively scarce. Such scarcity mainly originates from the difficulty in finding suitable material and rather narrow range of rock magnetic criteria required for reliable paleointensity work [1,2].

Regardless of the target material, the most reliable paleointensity technique is Thellier-type technique (e.g., [3–5]) where samples are subjected to double heatings. While each method uses different heating sequences (see [6] for detailed discussions), the fundamental principle is the same: the ratio of natural remanent magnetization (NRM) to partial thermoremanent magnetization (pTRM) should remain constant throughout entire heating steps unless there is alteration. When rocks or meteorites contain unstable material under heating [7,8], an alternative normalization technique with no heating is worthy for consideration.

The first alternative normalization technique involves relative comparison of intensity between anhysteretic

E-mail address: yjyu@ucsd.edu.

0012-821X/$ - see front matter © 2006 Elsevier B.V. All rights reserved.
doi:10.1016/j.epsl.2006.07.027

remanent magnetization (ARM) and thermoremanent magnetization (TRM) and/or their alternating-field (AF) demagnetization spectra. In the past, paleointensity determinations based on the ratio "*R*" of TRM/ARM intensities were widely used to estimate the lunar paleofield intensity (e.g., [9–14]). However, experimentally determined "*R*" values are inconsistent, the uncertainty being often as large as an order of magnitude [15]. It is worthy of note that the ARM intensity is dependent on the instrument [16] as well as on the decay-rate of AF [17]. Nonetheless Thellier experiments on the lunar samples yielded wide spectrum of varying paleointensities (e.g., [18,19]), and often show the evidence of self-reversal (e.g., [20]).

A second alternative technique involves relative comparisons of intensity between saturation isothermal remanent magnetization (SIRM) and NRM and/or their AF spectra. This NRM/SIRM technique was initially suggested to represent the efficiency of magnetization in a system with a value in the order of 10^{-2} [21]. In particular, the NRM versus SIRM demagnetization plot is practically useful in resolving multi-component NRM [22]. The ratio of NRM/SIRM has been applied for the extraterrestrial material to make an inference on the magnetic field intensity of the planetary body [23–30].

The present study was intended to test whether the TRM/SIRM ratio of magnetite is truly grain-size independent and stable during demagnetization. In addition, a quantitative guideline on the accuracy of the TRM/SIRM ratio will be provided.

2. TRM/SIRM

According to the thermal fluctuation theory for an ensemble of randomly oriented non-interacting uniaxial single-domain (SD) grains [31,32], TRM/SIRM ratio can be expressed as follows:

$$\frac{M_{\mathrm{trm}}(\boldsymbol{B}_0)}{M_{\mathrm{rs}}} = \tanh[VM_{\mathrm{s}}(T_{\mathrm{B}})\boldsymbol{B}_0/kT_{\mathrm{B}}]$$

in which V is grain volume, M_{s} is spontaneous magnetization (=480 kA/m for magnetite at room temperature), T_{B} is blocking temperature, $\boldsymbol{B}_0$ is the applied field, and k is the Boltzmann's constant. TRM ($\boldsymbol{B}_0$)/SIRM curves slowly increasing as the $\boldsymbol{B}_0$ increases (Fig. 1a). As expected from the equation, it reaches saturation at smaller field $\boldsymbol{B}_0$ as the grain-size of magnetite increases (Fig. 1a). For the values of $\boldsymbol{B}_0$ similar to those of historical terrestrial field (<0.1 mT), TRM/SIRM is linearly proportional to $\boldsymbol{B}_0$ except for grains>100 nm (Fig. 1b). This simple mathematical calculation clearly indicates that the TRM/SIRM ratio depends on the grain-size of magnetite as well as on the intensity of $\boldsymbol{B}_0$ (Fig. 1). It is fair to mention that the original Neel's SD theory requires modification to adequately explain TRM acquisition curves [33]. However, the grain-size dependence and field independence of TRM/SIRM is still evident in all variations of SD theory and observed data (see [33] for detailed discussions and references therein).

To test the grain-size dependence of TRM/SIRM and the stability of TRM/SIRM against demagnetization, we used eight commercial synthetic magnetite (Fe_3O_4) powders whose mean grain diameters ranged from 65 nm to 18.3 μm (Table 1). Grain diameters and shapes were previously determined (see [34] for details) under the microscope. At first, powders were dispersed in a matrix of CaF_2. Then, cylindrical pellets of powders (8.8 mm

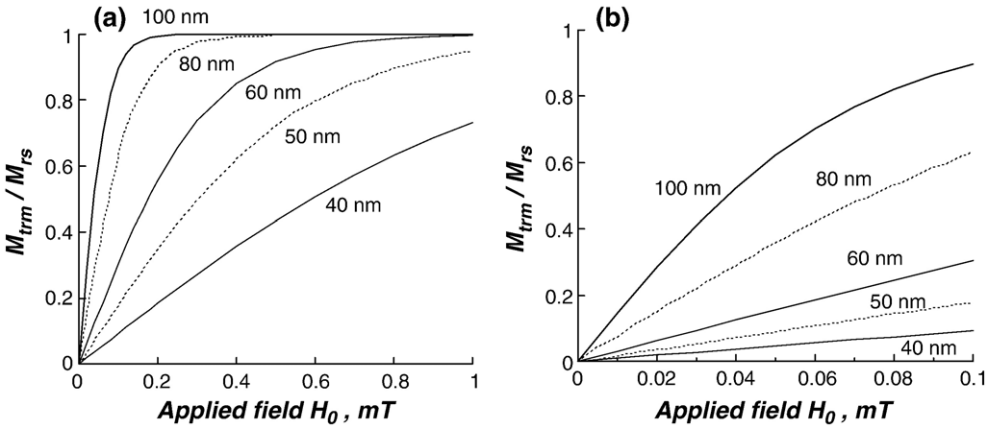

Fig. 1. (a) Theoretical calculation [31] of the TRM/SIRM ratio as a function of $\boldsymbol{B}_0$. The rapid rise in larger magnetite grains contrasts with the slow linear increase in 40 nm magnetite. M_{trm} and M_{rs} represent thermoremanent magnetization (TRM) and saturation isothermal remanent magnetization (SIRM), respectively (b) An amplified TRM/SIRM ratio in the range of historic Earth magnetic field intensity (<0.1 mT).

Table 1
Physical and magnetic properties of synthetic magnetites

Powder	d (μm)	q, aspect ratio	TRM (mA/m)	SIRM (A/m)	TRM/SIRM
4000	0.065	1.48	91.46	2.709	0.0338
5099	0.21	1.44	92.00	1.740	0.0529
Mapico	0.24	1.29	35.67	0.521	0.0684
5000	0.34	1.65	40.29	1.134	0.0355
112978	0.44	1.33	41.66	1.102	0.0378
3006	1.06	1.62	28.84	0.994	0.0290
112982	16.9	1.61	15.25	1.014	0.0150
041183	18.3	1.57	15.11	0.930	0.0162

Powders 4000, 5000, 112978, 3006, and 112982 are from the Wright Company. Powders 5099 and Mapico are the products of Pfizer and Mapico Companies. d is the estimated grain diameter and q is the average axial ratio. Size distribution was determined by counting individual grains from at least six different SEM photos per powder. See Yu et al., [34] for details. TRMs were produced by cooling from 600 °C in a steady field of 50 μT. The SIRM was produced by exposing samples in a field of 1 T.

diameter and 8.6 mm height) were tightly wrapped with quartz wool inside the quartz capsules, which were then sealed under vacuum and annealed for 6 h at 650 °C to stabilize the magnetic properties. TRMs were produced by cooling from 600 °C in a steady field $\boldsymbol{B}_0$ of 50 μT. The SIRM was produced by exposing samples in a field of 1 T using ASC-10 impulse magnetizer.

As expected from the theory, the TRM/SIRM ratio is far from being constant (Fig. 2). Instead, a pronounced grain-size dependence is observed (Fig. 2a) when compiled with other available data [33,35–37] (Table 2). Because other studies used different magnitude of $\boldsymbol{B}_0$ in producing TRMs (Table 2), it is necessary to estimate corrected TRM/SIRM ratio for $\boldsymbol{B}_0 = 50$ μT (Fig. 2b). This approximation assumes a linear field dependence of TRM in magnetite [32]. Whether corrected or not, values of TRM/SIRM are widely dispersed with maximum around 0.2 μm and minimum around 2–10 μm (Fig. 2a). In particular, a strong peak around 0.2 μm is unprecedented, as observed in the TRM/ARM ratio [33,38]. It is plausible that domains states of magnetite would be quite different between thermally treated TRM (e.g., two domains) and field-treated ARM or SIRM (e.g., vortex) [33,39,40]. There exists more than an order of difference in the TRM/SIRM ratio of magnetite (Fig. 2), suggesting that a strong constraint on the grain-size characterization is required if TRM/SIRM is applied for a paleointensity proxy in planetary magnetism.

Meteorites often exhibit composite magnetic vector (e.g., [41–43]). There are three potential sources that could influence the primary NRM in meteorites. First, most meteorites usually experience at least two shocking events: initial ejection from the mother planetary body and the later terrestrial entrance. Both events could influence the NRM because of the heat associated with substantial shock pressures (e.g., [44]). Second, a shock hardened remanence can be acquired in a strong local plasma even without thermal effects. Third, most documented meteorites were exposed to earth magnetic field for some time after their fall, possibly acquired viscous isothermal remanence. In practice, it is common to observe more than two magnetic components during demagnetization of NRM in lunar rocks (e.g., [7,18]) and in Martian meteorites (e.g., [41–43]).

To better handle such a composite NRM, partial AF demagnetization would be useful in resolving multi-component NRM. Then, it is curious whether TRM/SIRM is

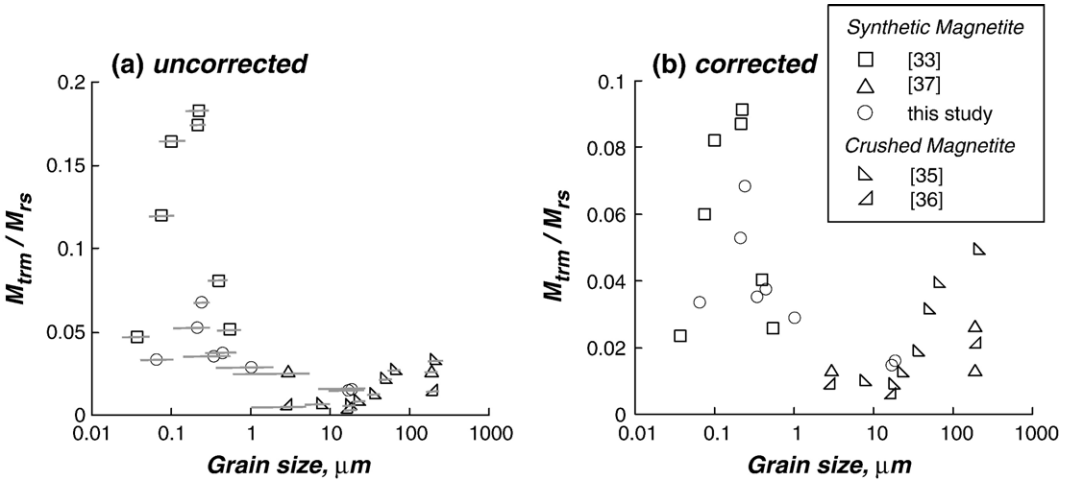

Fig. 2. The TRM/SIRM ratio as a function of magnetite grain size. (a) uncorrected TRM/SIRM as in Table 2. (b) Values of TRM/SIRM were corrected for $\boldsymbol{B}_0 = 50$ μT by assuming a linear field dependence of TRM in magnetite. In the present study, TRMs were produced by cooling from 600 °C in a steady field $\boldsymbol{B}_0$ of 50 μT. The SIRM was produced by exposing samples in a field of 1 T. Whether corrected or not, values of TRM/SIRM are widely dispersed with maximum around 0.2 μm and minimum around 2–10 μm.

Table 2
Compilation of the TRM/SIRM ratio

References	Grain size	TRM/SIRM	B_0 for TRM (μT)
[33]	37 nm (D4)	0.047	100
	76 nm (D3)	0.120	100
	100 nm (D2)	0.164	100
	220 nm (D1)	0.183	100
	215 nm (A1)	0.174	100
	390 nm (A2)	0.081	100
	540 nm (A3)	0.052	100
[35]	150–250 μm	0.0341	35
	55–75 μm	0.0278	35
	40–55 μm	0.0224	35
	30–40 μm	0.0135	35
	25–30 μm	0.0091	35
	15–20 μm	0.0064	35
	5–10 μm	0.0073	35
[36]	150–250 μm	0.0151	35
	15–20 μm	0.0045	35
	<5 μm	0.0066	35
[37]	3.0 μm	0.0265	100
	190.0 μm	0.0263	100

[33]: Dunlop and Argyle (1997); [35]: Hartstra (1982); [36]: Hartstra (1983); [37] Muxworthy and McClelland (2000); TRM: thermoremanent magnetization; SIRM: saturation isothermal remanent magnetization.

stable against AF demagnetization. Recent reassessments of the TRM/SIRM technique uses derivatives of AF demagnetized NRM and SIRM, which allow vectorial handling of data [27,29,45]. While these recent achievements provide practical tool in checking the robustness of the TRM/SIRM technique, it is still worth examining the stability of TRM/SIRM ratio during AF demagnetization. To test whether the TRM/SIRM ratio remains constant, stepwise AF demagnetization was carried out on TRM and SIRM respectively, using the Molspin AF demagnetizer at 2.5, 5, 7.5, 10, 15, 20, 25, 30, 35, 40, and 50 mT. We then compared values of TRM/SIRM as a function of peak AF.

The TRM/SIRM ratio increases as the AF increases for SD and pseudo-single-domain (PSD) magnetite (Fig. 3a). On the contrary, multidomain (MD) magnetite shows nearly constant TRM/SIRM ratio throughout entire AF steps (Fig. 3a). While the SD and PSD magnetites show a contrasting difference in AF demagnetization spectra between TRM and SIRM (Fig. 3b, c), MD magnetite shares similar AF demagnetization pattern between TRM and SIRM (Fig. 3d).

3. Calibrating the TRM/SIRM technique

3.1. Reliability of TRM/SIRM technique

In Section 2, on the basis of fundamental rock magnetic tests, two interesting observations are made. First, the TRM/SIRM ratio is dependent on the grain-size of magnetite (Fig. 2). Second, TRM/SIRM increases as the peak AF increases for fine-grained magnetite (Fig. 3). In particular, the second aspect is critical in reality when partial AF demagnetization of NRM is inevitable. Note also that the elongation of magnetite grains has a tendency in increasing the TRM/SIRM ratio [46,47]. In addition to these observations, natural meteorites may pose more complexities including various magnetic compositions other than magnetite, complicated NRM vector with more than two components, and no available a priori information on the planetary magnetic field intensity. To this end, it is likely that the TRM/SIRM technique can only suggest crude estimations on the planetary magnetic field intensity. As a matter of fact, even the most advanced TRM/SIRM technique (e.g., [29]) acknowledged a factor of two uncertainties.

Despite various sources of uncertainties in estimating the ancient planetary magnetic field intensity, the TRM/SIRM technique still deserves further investigation because of its practical merit. In practice, applying the Thellier-type technique on meteorites is extremely difficult because of two well-known reasons. First, most extraterrestrial materials easily alter during heating (e.g., [7,18,21,43]). Thus, even a very delicate experimental design with double-buffer-encapsulation of meteorites in quartz tubing [48] cannot prevent the alteration. Second, curation regulation on meteorites is very stringent considering the fact that the heated magnetic phases cannot be re-used in other scientific investigation. Therefore, an alternative non-heating technique deserves practical attention.

How accurately can NRM/SIRM technique determine the ancient planetary magnetic field intensity? In a recent study, Kletetschka et al. [28] suggested $\boldsymbol{B}$ (in Tesla) = ~ 0.003 × (NRM/SIRM) as a calibration factor. For instance, $\boldsymbol{B}$ = 90 μT is estimated for the NRM/SIRM ratio of 0.03 [28]. However, such conversion is likely to be ambiguous because NRM of meteorite can be multivectorial and NRM carrier is not always magnetite. Note that it has been observed that various magnetic compositions can contribute to the NRM of meteorites. For instance, iron-oxides, iron-sulfides, and Cr–Fe-rich spinels have been found to be responsible for the stable remanence in Martian meteorites (e.g., [8,41–43,49–56]). In the calibrations of the lunar samples, the TRM/SIRM ratio varied with field (from more than an order of magnitude) and sample [57,58]. Due to such inherent sources of ambiguities, Gattacceca and Rochette [29] wisely proposed a factor of two uncertainties in using the NRM/SIRM method.

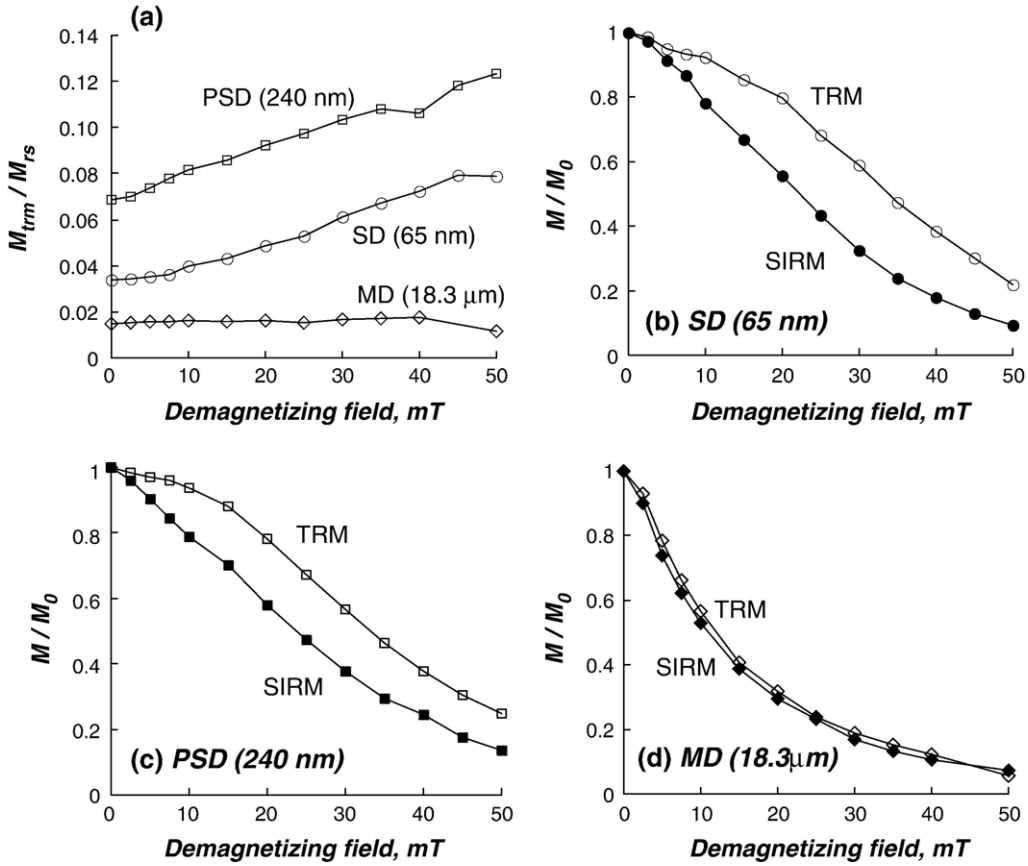

Fig. 3. (a) Testing the stability of the TRM/SIRM ratio as a function of AF. M: Magnetization; M_0: initial remanence (=TRM or SIRM). The ratio increases as the AF increases for SD and PSD. AF demagnetization of TRM and SIRM for (b) SD, (c) PSD, and (d) MD. For SD and PSD, TRM is more resistant to AF demagnetization than the SIRM, resulting in an apparent increase in the TRM/SIRM ratio in (a).

3.2. Paleointensity samples

In order to provide a better calibrating relation, a simple paleointensity test was carried out using historic terrestrial lava. For convenience, the present study considers the simplest case where univectorial NRM is carried by a single composition of magnetic mineral (low-Ti titanomagnetite). Located in Mountain Sakurajima, Japan, Showa lava erupted in 1946 with pyroclastic materials [59]. The Showa lava mostly has a thick pumice deposits whose bottoms consist of dark andesitic welded tuffs [59]. We used 12 unoriented block samples collected from the bottom portion of dark-brown Showa lava in the present study. Samples from the top or intermediate portion were not used because they contain magnetic material with lower Curie points [60].

The Showa lava perfectly fits with the objective of the present study. The Showa lava revealed successful paleointensity in a previous study [60]. The Showa lava also showed a univectorial decay of NRM during demagnetization, suggesting that the NRM was not affected by later magnetic or thermal activity [60]. In other words, NRM of Showa lava is purely TRM.

3.3. Paleointensity determination

Strong-field hysteresis and the temperature dependence of weak-field susceptibility were measured to characterize the rock magnetic properties of selected chips. To estimate Curie points, the temperature dependence of weak-field magnetic susceptibility was determined in air at the Institute for Rock Magnetism, University of Minnesota. A typical example whose sister chips yielded successful Thellier results (see Section 3.4) shows reversible curves (Fig. 4a). The estimated Curie point is ~560 °C, indicating the presence of low-Ti titanomagnetite (Fig. 4a).

Room temperature hysteresis measurements in a maximum field of 1.0 T were performed on an alternating gradient force magnetometer. Hysteresis loops were obtained for 36 chips, three from each block sample. All

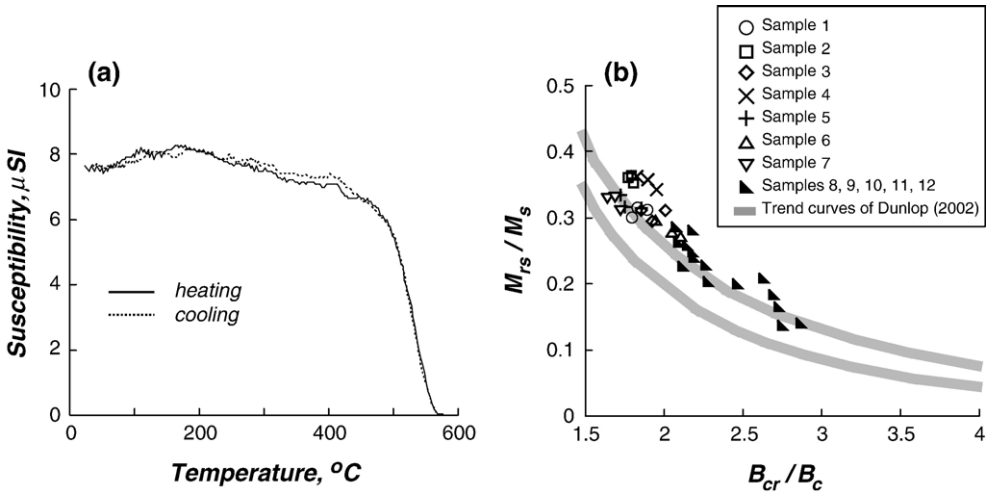

Fig. 4. (a) Example of nearly reversible thermomagnetic curves. Solid (dashed) lines are for heating (cooling). (b) Day plot [61] for Showa lava. Results fall in the PSD range or match well with the SD+MD mixing trend curves [62].

loops were corrected for paramagnetism. Values of saturation magnetization (M_s), saturation remanence (M_{rs}), and coercive force (B_c) were determined from hysteresis loops. Values of remanence coercivity (B_{cr}) were obtained from back-field measurements. The ratio of M_{rs}/M_s and B_{cr}/B_c of the 36 chips lie in the PSD range according to the criteria of Day et al. [61] or in the trend curves defined by Dunlop [62] (Fig. 4b). Note that values of M_{rs}/M_s are generally higher ($M_{rs}/M_s > 0.272$) for chips from samples 1–7 than those from samples 8–12 whose sister chips yielded MD behavior during Thellier run (see Section 3.4) (Fig. 4b).

In order to retrieve absolute paleointensity information, a Coe-modified Thellier method [4] was applied for 60 chips (five each per block sample) of Showa lava. After the first (zero-field) heating-cooling step to temperature T_i, the remanence was measured and the NRM lost was calculated. The second heating-cooling step to temperature T_i was in $\boldsymbol{B}=40$ μT along the cylindrical z-axis of the specimen. Subtraction of the first- and second-step remanences gave the partial TRM (pTRM) acquired at T_i. Double heatings were carried out at 200, 400, 452, 471, 492, 512, 526, 542, 551, and 565 °C. We made pTRM checks at 400, 471, 512, and 542 °C. Throughout all heat treatments, temperatures were reproducible within 1.3 °C. Following the paleointensity experiments, the anisotropy of anhysteretic remanent magnetization (AARM) tensor was defined [63] for each accepted specimen. The AARM tensor was determined by measuring ARM along nine different positions as in Jelinek [64]. The effects of remanence anisotropy were then corrected using AARM tensor [65].

Paleointensity results were accepted only if they satisfied the following selection criteria.

1. Because NRM is purely TRM, the "entire" Arai plot [66] must be linear.

Table 3
Paleointensity results

Specimen	N	$\boldsymbol{B}$, d$\boldsymbol{B}$ (μT)	f	g	q	S'
SH1A	11	43.74 (0.59)	1.00	0.89	65.2	0.427
SH1B	11	46.00 (0.77)	1.00	0.88	52.9	1.548
SH1C	11	45.87 (0.63)	1.01	0.89	65.1	0.857
SH1D	11	46.10 (0.77)	1.01	0.89	53.9	1.499
SH1E	11	47.01 (0.67)	1.01	0.88	62.3	1.027
SH2A	11	46.13 (0.64)	1.01	0.88	64.3	1.001
SH2B	11	45.02 (0.75)	1.02	0.89	54.1	1.436
SH2C	11	46.21 (0.64)	1.01	0.88	64.2	0.377
SH2D	11	47.55 (0.66)	1.01	0.89	64.6	0.624
SH2E	11	46.00 (0.67)	1.02	0.89	62.3	1.157
SH3B	11	47.23 (0.64)	1.01	0.89	65.9	0.617
SH3C	11	46.40 (0.63)	1.01	0.89	66.2	0.664
SH3D	11	45.46 (0.59)	1.01	0.89	69.1	1.014
SH4A	11	46.06 (0.62)	1.02	0.89	67.5	0.496
SH4D	11	48.56 (0.71)	1.01	0.88	60.7	0.455
SH5A	11	44.48 (0.62)	1.00	0.88	63.3	0.293
SH5E	11	46.67 (0.66)	1.01	0.88	63.0	0.152
SH6D	11	46.00 (0.64)	1.01	0.88	63.8	0.379
SH6E	11	46.69 (0.64)	1.02	0.88	64.8	0.422
SH7A	11	46.24 (0.74)	1.01	0.88	55.7	1.407
SH7B	11	44.59 (0.60)	1.00	0.89	66.2	0.104
Mean		46.10 (1.08)				

N is the number of datapoints used in paleointensity estimation; f, g, and q are NRM fraction, gap factor, and quality factor of Coe et al. [67]; S' is the goodness of the fit defined by Yu et al. [68].

2. Demagnetization of NRM must be univectorial.
3. All the pTRM checks must agree with the original pTRMs within 5%.
4. Quality of statistical assessment must pass the commonly used guideline [67] as well as a more stringent goodness of the fit test [68] (Table 3).

A typical successful paleointensity result displays a perfectly linear Arai plot from T_0 to T_c (Fig. 5a). For accepted samples, the pTRM checks reproduce the original pTRMs (Fig. 5a) and the NRM shows a univectorial decay (Fig. 5b). As briefly mentioned in Section 3.2 (Fig. 4), all the chips from samples 8–12 showed MD-behavior with convex-down features in Arai-plot (Fig. 5c). Due to their severe non-linearity, no acceptable paleointensity was observed from these samples (Fig. 5c). Among remaining 35 chips from samples 1–7, 21 chips yielded acceptable results while 14 chips were rejected. These rejected 14 chips failed pTRM checks (Fig. 5d).

The estimated paleointensity of Showa lava from the Thellier experiment is 46.1±1.1 μT (Table 3), statistically indistinguishable from the previously determined paleointensity of 45.5±2.2 μT [60]. These paleointensity determinations agree well with the actual magnetic field intensity observation of 46.80 μT in 1959 AD from the Aso Volcanological Observatory in Japan (courtesy of World Data Center for Geomagnetism, Kyoto, Japan at http://swdcwww.kugi.kyoto-u.ac.jp).

3.4. Calibrating the TRM/SIRM technique

Because all the chips in samples 1 and 2 yielded reliable paleointensities during Thellier experiments (Table 3), further testings used additional sister chips retrieved from these two samples. From each sample, 21 additional chips were retrieved for the NRM/SIRM measurements. Due to irregular shapes, chips were encapsulated in a cylindrical glass-tube. First, NRM of 42 chips were measured. Second, SIRM was produced by

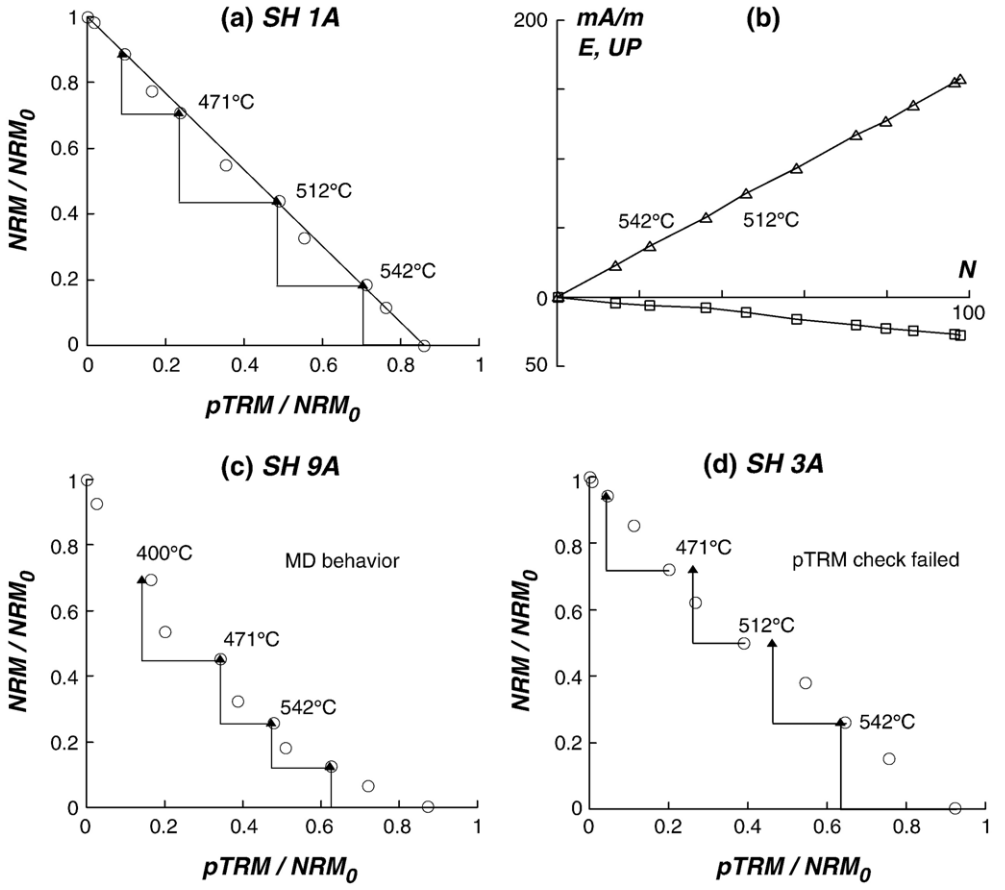

Fig. 5. (a) A typical example of successful paleointensity determination. All the datapoints lie along a straight line whose slope is proportional to the paleointensity. Open circles: NRM lost versus pTRM acquisition; solid triangles: pTRM checks. (b) NRM shows a univectorial decay in vector projections. (c) SH9A shows severe convex-down non-linear features in Arai-plot. (d) Two pTRM checks at 471 °C and 512 °C were failed for SH3A.

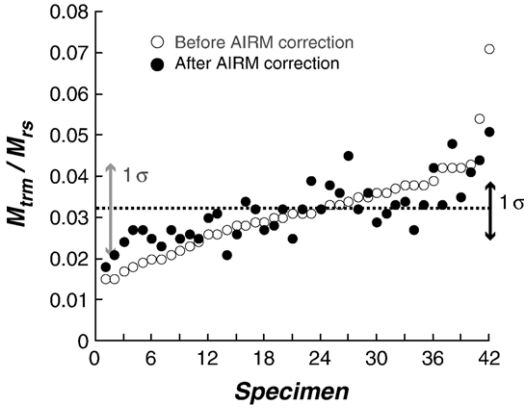

Fig. 6. The NRM/SIRM ratio for Showa lava erupted in 1946. The NRM/SIRM testing yielded 0.031±0.011 without AIRM correction and 0.032±0.007 with AIRM correction. Specimen numbers are sorted out in ascending order.

applying a field of 1.0 T along the cylindrical axis of the sample-tube. However, this typical sequence of NRM/SIRM experiment is possibly sensitive to the inherent magnetic fabric anisotropy or sample shape anisotropy because SIRM is produced only along a single axis. In order to correct any such anisotropy, the anisotropy of isothermal remanent magnetization (AIRM) tensor was defined [63] for all 42 chips. The AIRM tensor was determined by measuring IRM along nine different positions as in Jelinek [64]. The effects of remanence anisotropy were then corrected using AIRM tensor [65].

The average NRM/SIRM ratio is 0.031±0.011 without AIRM correction and 0.032±0.007 with AIRM correction (Fig. 6). While the AIRM correction does not affect the mean value, it certainly reduced the scattering in the distribution of data-points (Fig. 6). For instance, the distribution of NRM/SIRM without AIRM correction is quite scattered with values from 0.015 to 0.071, but 0.018–0.051 after AIRM correction (Fig. 6).

4. Discussion

One fundamental assumption in using normalization technique as a mean to estimate the ancient magnetic field intensity is that the normalization must be grain-size independent of magnetic material. For example, there is a stringent constraint on grain-size proxy in relative paleointensity determination where ARM or SIRM is frequently used as a normalizer (e.g., [69]). While the Fuller et al. [22] clearly pointed out grain-size dependence of NRM/SIRM in their work, later successors who used NRM/SIRM techniques merely assumed a grain-size independence. In a recent study, Kletetschka et al. [28] investigated Murchison meteorites and documented a grain-size independence in their NRMs. Perhaps the magnetic carrier of Murchison is uniform in terms of its magnetic grain-size. We tested whether the TRM/SIRM ratio is truly independent from the grain-size of magnetite. Compilation of the measured values of TRM/SIRM displays more than an order of difference between the maximum and the minimum values (Fig. 2). Thus, it is recommended that a strong constraint on magnetic grain-size is required if TRM/SIRM is applied for a paleointensity proxy in planetary magnetism.

Stability of the TRM/SIRM ratio against AF demagnetization was also tested. In practice, it is common to observe composite NRMs in extraterrestrial materials (e.g., [7,18,41–43]). For meteorites, such multi-component NRMs are natural because they experience at least two major shocking events (ejection and terrestrial entrance) accompanying high shock pressures and heat [44] that might influence the primary NRM. In addition, some meteorites were found after long exposure to earth magnetic field after their fall. If so, partial AF demagnetization is necessary to isolate the primary NRM. Unfortunately, the TRM/SIRM ratio increases as the peak AF increases for fine-grained magnetite (Fig. 3a). The TRM/SIRM ratio remains constant only for MD, the material usually unsuitable in paleointensity work (Fig. 3a). For SD and PSD, TRM/SIRM increases as the peak AF increases because TRM is more resistant to demagnetization than the SIRM (Fig. 3b, c). On the other hand, TRM/SIRM remains constant for MD because TRM and SIRM share similar AF demagnetization spectra (Fig. 3d). In fact, it is common to observe a harder TRM than SIRM in fine-grain titanomagnetite (e.g., [70–72]). Overall, it is likely that applying partial AF demagnetization on TRM (or NRM in nature) would overestimate the true TRM/SIRM ratio if NRM is carried by fine-grained magnetite (Fig. 3).

What would be a conversion relation between the TRM/SIRM ratio and the Thellier paleointensity determination? To correlate the TRM/SIRM ratio with the Thellier estimation, we used Showa lava erupted in 1946. The Showa lava fits our purpose in various aspects including univectorial primary magnetization, single composition of magnetic mineralogy (low-Ti titanomagnetite), successful paleointensity work in a previous study, and available magnetic field intensity information from the observatory. The mean paleointensity from Thellier experiments was 46.1±1.1 μT, in excellent agreement with the measured value of 46.80 μT in 1959 from the adjacent magnetic observatory (http://swdcwww.kugi.kyoto-u.ac.jp). The NRM/SIRM testing yielded 0.031±0.011 without AIRM correction and 0.032±0.007 with AIRM correction (Fig. 6). In practice, it is strongly recommended that AIRM correction is necessary because meteoritic chips may

possess magnetic fabric. In addition, it is likely that the textures of lava flows often contain magnetic grains in skeleton shapes. In the future, the NRM/SIRM ratio of 0.032 ± 0.007 can be correlated with 46.80 μT if NRM is carried by low-Ti titanomagnetite. This conversion rate is about half to Murchison data [28] and ~1/3 to lunar data [57,58]. Such discrepancy may result from the complex nature of NRMs (e.g., composite NRM vector, various compositions of NRM carriers) and lack of anisotropy correction in earlier studies. It is also fair to mention that most Thellier paleointensity works yield higher uncertainties than reported here due to complex nature of NRM. Note that it remains to be shown whether the same rate of conversion is validated for other compositions of magnetic minerals.

How accurately can NRM/SIRM technique determine the ancient planetary magnetic field intensity? In the present study, the ideal case of NRM was tested where it is univectorial, it is purely TRM, and it is carried by a single composition of magnetic mineralogy (Fig. 5). Despite such simplicities in experimental designs, the TRM/SIRM technique displayed large scatters (Fig. 6). Although the AIRM correction reduced the scatters in data distribution to some degree (Fig. 6), the $\sigma/\boldsymbol{B}_{\mathrm{mean}}$ of TRM/SIRM method (=22%) is 10 times larger than that of Thellier work (=2.3%) (Table 3). Therefore, the NRM/SIRM ratio can only be used as a crude estimation on the absolute planetary magnetic field intensity.

Is the NRM/SIRM technique useful? The TRM/SIRM ratio is grain-size dependent for magnetite (Fig. 2). It is also not constant to partial AF demagnetization for fine-grained magnetite (Fig. 3). Furthermore, meteorites and rocks collected from other planets (e.g., lunar rocks; Martian soils in the near future) may contain various compositions other than magnetite including Fe–Cr-rich spinel [41,43], hematite [73,74], hemoilmenite [75,76], kamacite [77,78], pyrrhotite [52,64], spinel [79], and titanohematite [80]. Despite such uncertainties, the TRM/SIRM ratio could be the only practical tool in approximately estimating the planetary field intensity because applying the Thellier-type technique on meteorites is extremely difficult due to easy alteration [7,18,43] and stringent curation regulation.

Acknowledgments

David J. Dunlop and Yasuo Miyabuchi provided fruitful discussions. Mike Fuller and two anonymous reviewers greatly improved the paper. Mike Jackson of the Institute for Rock Magnetism (IRM) provided tremendous help with the rock magnetic measurements. The Keck Foundation, the National Science Foundation, Earth Sciences Division, and the University of Minnesota provide funding for the IRM.

References

[1] P. Selkin, L. Tauxe, Long-term variations in paleointensity, Philos. Trans. R. Soc. Lond., A 358 (2000) 1065–1088.
[2] J.-P. Valet, Time variations in geomagnetic intensity, Rev. Geophys. 41 (1) (2003) 1004, doi:10.1029/2001RG000104.
[3] E. Thellier, O. Thellier, Sur l'intensité du champ magnétique terrestre dans le passé historique et géologique, Ann. Géophys. 15 (1959) 285–376.
[4] R.S. Coe, Paleointensities of the Earth's magnetic field determined from Tertiary and Quaternary rocks, J. Geophys. Res. 72 (1967) 3247–3262.
[5] M.J. Aitken, A.L. Allsop, G.D. Bussell, M.B. Winter, Determination of the intensity of the Earth's magnetic field during archaeological times: reliability of the Thellier technique, Rev. Geophys. 26 (1988) 3–12.
[6] Y. Yu, L. Tauxe, A. Genevey, Toward an optimal geomagnetic field intensity determination technique, Geochem. Geophys. Geosys. 5 (2) (2004) Q02H07, doi:10.1029/2003GC000630.
[7] M. Fuller, Lunar magnetism, Rev. Geophys. Space Phys. 12 (1974) 23–70.
[8] S.M. Cisowski, Magnetic studies on Shergotty and other SNC meteorites, Geochim. Cosmochim. Acta 50 (1986) 1043–1948.
[9] H. Markert, F. Heller, Determination of paleointensities of the geomagnetic field from anhysteretic remanent magnetization, Phys. Status Solid., A 14 (1972) K47.
[10] D.W. Collinson, A. Stephenson, S.K. Runcorn, Magnetic properties of Apollo 15 and 16 rocks, Geochim. Cosmochim. Acta 37 (4) (1973) 2963–2976.
[11] S.K. Banerjee, J.P. Mellema, A new method for the determination of paleointensity from the ARM properties of rocks, Earth Planet. Sci. Lett. 23 (1974) 177–184.
[12] A. Stephenson, D.W. Collinson, Lunar magnetic field paleointensities determined by an anhysteretic remanent magnetization method, Earth Planet. Sci. Lett. 23 (1974) 220–228.
[13] O.L. Bagina, G.N. Petrova, Determination of paleomagnetic field intensity using anhysteretic remanent magnetization, Phys. Earth Planet. Inter. 13 (1977) 363–367.
[14] N. Sugiura, D.W. Strangway, Magnetic paleointensity determination on lunar sample 62235, J. Geophys. Res. 88 (1983) A684–A690.
[15] M.E. Bailey, D.J. Dunlop, On the use of anhysteretic remanent magnetization in paleointensity determination, Phys. Earth Planet. Inter. 13 (1977) 360–362.
[16] L. Sagnotti, P. Rochette, M. Jackson, F. Vadeboin, J. Dinares-Turell, A. Winkler, Magnet Science team, inter-laboratory calibration of low-filed magnetic and anhysteretic susceptibility measurements, Phys. Earth Planet. Inter. 138 (2003) 25–38.
[17] Y. Yu, D.J. Dunlop, Decay-rate dependence of anhysteretic remanence: fundamental origin and paleomagnetic applications, J. Geophys. Res. 108 (B12) (2003) 2550, doi:10.1029/2003JB002589.
[18] G.W. Pearce, G.S. Hoye, D.W. Strangway, B.M. Walker, L.A. Taylor, Some complexities in the determination of lunar paleointensities, Geochim. Cosmochim. Acta 40 (1976) 3271–3297.
[19] N. Sugiura, D.W. Strangway, Comparisons of magnetic paleointensity methods using a lunar sample, Proc. 11th Lonmar Sci. Conf., Pergamon, 1980, pp. 1801–1813.

[20] S.K. Chowdhary, D.W. Collinson, A. Stephenson, S.K. Runcorn, Further investigations into lunar paleointensity determination, Phys. Earth Planet. Inter. 49 (1987) 133–141.
[21] S. Cisowski, M. Fuller, Lunar paleointensities via the IRMs normalization method and the early history of the moon, in: W.K. Hartmann, R.J. Phillips, G.J. Taylor (Eds.), Origin of the Moon, Lunar and Planetary Institute, Houston, 1986, pp. 411–424.
[22] M. Fuller, S. Cisowski, M. Hart, R. Haston, E. Schmidtke, NRM: IRM(s) demagnetization plots: an aid to the interpretation of natural remanent magnetization, Geophys. Res. Lett. 15 (5) (1988) 518–521.
[23] P. Wasilewski, Magnetization of small iron–nickel spheres, Phys. Earth Planet. Inter. 26 (1981) 149–161.
[24] P. Wasilewski, G. Kletetschka, Lodestone: natures only permanent magnet—what it is and how it gets charged, Geophys. Res. Lett. 26 (15) (1999) 2275–2278.
[25] P. Wasilewski, T. Dickinson, Aspects of the validation of magnetic remanence in meteorites, Meteorit. Planet. Sci. 35 (2000) 537–544.
[26] P. Wasilewski, M.H. Acuna, G. Kletetschka, 433 Eros: problems with the meteorite magnetism record in attempting an asteroid match, Meteorit. Planet. Sci. 37 (2002) 937–950.
[27] J. Gattacceca, P. Rochette, M. Bouot-Denise, Magnetic properties of a freshly fallen LL ordinary chondrite: the Bensour meteorite, Phys. Earth Planet. Inter. 140 (2003) 343–358.
[28] G. Kletetschka, T. Kohout, P.J. Wasilewski, Magnetic remanence in the Murchison meteorite, Meteorit. Planet. Sci. 38 (2003) 399–405.
[29] J. Gattacceca, P. Rochette, Toward a robust normalized magnetic paleointensity method applied to meteorites, Earth Planet. Sci. Lett. 227 (2004) 377–393.
[30] G. Kletetschka, M.H. Acuna, T. Kohout, P.J. Wasilewski, J.E.P. Connerney, An empirical scaling law for acquisition of thermoremanent magnetization, Earth Planet. Sci. Lett. 226 (2004) 521–528.
[31] L. Néel, Théorie du traînage magnétique des ferromagnéniques en grains fins avec applications aux terres cuites, Ann. Géophys. 5 (1949) 99–136.
[32] D.J. Dunlop, Ö. Özdemir, Rock Magnetism: Fundamentals and Frontiers, Cambridge University Press, New York, 1997.
[33] D.J. Dunlop, K.S. Argyle, Thermoremanence, anhysteretic remanence, and susceptibility of submicron magnetites: nonlinear field dependence and variation with grain size, J. Geophys. Res. 102 (B9) (1997) 20199–20210.
[34] Y. Yu, D.J. Dunlop, Ö. Özdemir, Partial anhysteretic remanent magnetization in magnetite. 1. Additivity, J. Geophys. Res. 107 (B10) (2002) 2244, doi:10.1029/2001JB001249.
[35] R.L. Hartstra, High-temperature characteristics of a natural titanomagnetite, Geophys. J. R. Astron. Soc. 71 (1982) 455–476.
[36] R.L. Hartstra, TRM, ARM, and I_{sr} of two natural magnetites of MD and PSD grain size, Geophys. J. R. Astron. Soc. 73 (1983) 719–737.
[37] A.R. Muxworthy, E. McClelland, The causes of low-temperature demagnetization of remanence in multidomain magnetite, Geophys. J. Int. 140 (2000) 132–146.
[38] Y. Yu, D.J. Dunlop, Ö. Özdemir, Are ARM and TRM analogs? Thellier analysis of ARM and pseudo-Thellier analysis of TRM, Earth Planet. Sci. Lett. 205 (2003) 325–336.
[39] S.L. Halgedahl, Magnetic domain patterns observed on synthetic Ti-rich titanomagnetites as a function of temperature and in states of thermoremanent magnetization, J. Geophys. Res. 96 (1991) 3943–3972.
[40] M. Winklehofer, K. Fabian, F. Heider, Magnetic blocking temperatures of magnetite calculated with a three-dimensional micromagnetic model, J. Geophys. Res. 102 (1997) 22695–22709.
[41] B.P. Weiss, J.L. Kirschvink, F.J. Baudenbacher, H. Vali, N.T. Peters, F.A. Macdonald, J.P. Wikswo, A low temperature transfer of ALH84001 from Mars to Earth, Science 290 (2000) 791–795.
[42] M. Antretter, M. Fuller, E. Scott, M. Jackson, B. Moskowitz, P. Solheid, Paleomagnetic record of Martian meteorite ALH84001, J. Geophys. Res. 108 (E6) (2003) 5049, doi:10.1029/2002JE001979.
[43] Y. Yu, J.S. Gee, Spinel in Martian meteorite SaU 008: implications for Martian magnetism, Earth Planet. Sci. Lett. 232 (2005) 287–294.
[44] L.E. Nyquist, D.D. Bogard, C.Y. Shih, A. Greshake, D. Stoffler, O. Eugster, Ages and geologic histories of Martian meteorites, Space Sci. Rev. 96 (2001) 105–164.
[45] V. Verrier, P. Rochette, Estimating peak currents at ground lightning impacts using remanent magnetization, Geophys. Res. Lett. 29 (18) (2002) 1867, doi:10.1029/2002GL015207.
[46] G. Kletetschka, M.H. Acuna, T. Kohout, P.J. Wasilewski, J.E.P. Connerney, An empirical scaling law for acquisition of thermoremanent magnetization, Earth Planet. Sci. Lett. 226 (2004) 521–528.
[47] G. Kletetschka, M.D. Fuller, T. Kohout, P.J. Wasilewski, E. Herrero-Bervera, N.F. Ness, M.H. Acuna, TRM in low magnetic fields: a minimum field that can be recorded by large multidomain grains, Phys. Earth Planet. Inter. 154 (2006) 290–298.
[48] L.A. Taylor, Paleointensity determinations at elevated temperatures: sample preparation technique, Proc. Lunar Planet. Sci. Conf. 10 (1979) 2183–2187.
[49] T.N. Nagata, Paleomagnetism of Antarctic achondrites, Mem. Natl. Inst. Polar Res., Spec. Issue 17 (1980) 233–242.
[50] D.W. Collinson, Magnetic properties of Antarctic shergottite meteorites EETA 79001 and ALHA 77005: possible relevance to a Martian magnetic field, Earth Planet. Sci. Lett. 77 (1986) 159–164.
[51] D.W. Collinson, Magnetic properties of Martian meteorites: implications for an ancient Martian magnetic field, Meteorit. Planet. Sci. 32 (1997) 803–811.
[52] J.L. Kirschvink, A.T. Maine, H. Vali, Paleomagnetic evidence of a low-temperature origin of carbonate in the Martian meteorite ALH84001, Science 275 (1997) 1629–1633.
[53] R.B. Hargraves, J.M. Knudsen, P. Bertelsen, W. Goetz, H.P. Gunnlaugsson, S.F. Hviid, M.B. Madsen, M. Olsen, Magnetic enhancement on the surface of Mars? J. Geophys. Res. 105 (E1) (2000) 1819–1827.
[54] P. Rochette, J.-P. Lorand, G. Fillion, V. Sautter, Pyrrhotite and the remanent magnetization on SNC meteorites: a changing perspective on Martian magnetism, Earth Planet. Sci. Lett. 190 (2001) 1–12.
[55] J. Shaw, M.J. Hill, S.J. Openshaw, Earth Planet. Sci. Lett. 190 (2001) 103–109.
[56] B.P. Weiss, H. Vali, F.J. Baudenbacher, J.L. Kirschvink, S.T. Stewart, D.L. Shuster, Earth Planet. Sci. Lett 201 (2002) 449–463.
[57] S. Cisowski, A review of lunar paleointensity data and implications for the origin of lunar magnetism, Proc. 13th Lunar Planet. Sci. Conf., J. Geophys. Res., vol. 88, 1983, pp. A691–A704.
[58] M. Fuller, S.M. Cisowski, Lunar paleomagnetism, in: J.A. Jacobs (Ed.), Geomagnetism, vol. 2, Academic Press, Toronto, 1987, pp. 307–455, Chapter 4.
[59] K. Ishihara, T. Takayama, Y. Tanaka, J. Hirabayashi, Lava flows at Sakurajima volcano (1), volume of the historic lava flows, Ann. Sisast. Prev. Res. Inst., Kyoto Univ., 24B-1, 1981, pp. 1–10.
[60] H. Tanaka, Paleointensities of the geomagnetic field determined from recent four lava flows of Sakurajima volcano, west Japan, J. Geomagn. Geoelectr. 32 (1980) 171–179.

[61] R. Day, M. Fuller, V.A. Schmidt, Hysteresis properties of titanomagnetites: grain-size and compositional dependence, Phys. Earth Planet. Inter. 13 (1977) 260–267.
[62] D.J. Dunlop, Theory and application of the Day plot. 1. Theoretical curves and tests using titanomagnetite data, J. Geophys. Res. 107 (B3) (2002) 2056, doi:10.1029/2001JB000486.
[63] C. McCabe, M. Jackson, B. Ellwood, Magnetic anisotropy in the Trenton Limestone: results of a new technique, anisotropy of anhysteretic susceptibility, Geophys. Res. Lett. 12 (6) (1985) 333–336.
[64] V. Jelinek, The statistical theory of measuring anisotropy of magnetic susceptibility and its application, Brno (1977) 87.
[65] P.A. Selkin, J.S. Gee, L. Tauxe, W.P. Meurer, A. Newell, The effect of remanence anisotropy on paleointensity estimates: a case study from the Archean Stillwater Complex, Earth Planet. Sci. Lett. 183 (2000) 403–416.
[66] T. Nagata, Y. Arai, K. Momose, Secular variation of the geomagnetic field total force during the last 5000 years, J. Geophys. Res. 68 (1963) 5277–5281.
[67] R.S. Coe, C.S. Gromme, E.A. Mankinen, Geomagnetic paleointensities from radiocarbon-dated lava flows on Hawaii and the question of the Pacific nondipole low, J. Geophys. Res. 83 (1978) 1740–1756.
[68] Y. Yu, D.J. Dunlop, L. Pavlish, M. Cooper, Archeomagnetism of Ontario potsherds from the last 2000 years, J. Geophys. Res. 105 (B8) (2000) 19419–19433.
[69] L. Tauxe, Sedimentary records of relative paleointensity of the geomagnetic field: theory and practice, Rev. Geophys. 31 (1993) 319–354.
[70] D.J. Dunlop, G.F. West, An experimental evaluation of single domain theories, Rev. Geophys. 7 (1969) 709–757.
[71] W. Lowrie, M. Fuller, On the alternating field demagnetization characteristics of multidomain thermoremanent magnetization in magnetite, J. Geophys. Res. 76 (1971) 6339–6350.
[72] Y. Yu, D.J. Dunlop, Ö. Özdemir, On the resolution of multivectorial remanences, Earth Planet. Sci. Lett. 208 (2003) 13–26.
[73] G. Kletetschka, P.J. Wasilewski, P.T. Taylor, Unique thermoremanent magnetization of multidomain hematite: implications for magnetic anomalies, Earth Planet. Sci. Lett. 176 (2000) 469–479.
[74] D.J. Dunlop, G. Kletetschka, Multidomain hematite: source of planetary magnetic anomalies? Geophys. Res. Lett. 28 (2001) 3345–3348.
[75] S.A. McEnroe, R.J. Harrison, P. Robinson, F. Langhorst, Nanoscale hematite–ilmenite lamellae in massive ilmenite rock: an example of 'Lamellar Magnetism' with implications for planetary magnetic anomalies, Geophys. J. Int. 151 (2002) 890–912.
[76] P. Robinson, R.J. Harrison, S.A. McEnroe, R.B. Hargraves, Lamellar magnetism in the hematite–ilmenite series as an explanation for strong remanent magnetization, Nature 418 (2002) 517–520.
[77] P. Wasilewski, Magnetization of small iron–nickel spheres, Phys. Earth Planet. Inter. 26 (1981) 149–161.
[78] T. Nagata, Meteorite magnetization and paleointensity, Adv. Space Res. 2 (1983) 55–63.
[79] A. Kontny, A.B. Woodland, M. Koch, Temperature-dependent magnetic susceptibility behaviour of spinelloid and spinel solid solutions in the systems Fe_2SiO_4–Fe_3O_4 and $(Fe,Mg)_{(2)}SiO_4$–Fe_3O_4, Phys. Chem. Miner. 31 (2004) 28–40.
[80] G. Kletetschka, P.J. Wasilewski, P.T. Taylor, The role of hematite–ilmenite solid solution in the production of magnetic anomalies in ground- and satellite-based data, Tectonophysics 347 (2002) 167–177.